



Cite this: *Phys. Chem. Chem. Phys.*,  
2016, 18, 18414

## Surface adsorption of sulfonated poly(phenylene sulfone)/C<sub>14</sub>TAB mixtures and its correlation with foam film stability

Martin Uhlig,<sup>a</sup> Reinhard Miller<sup>b</sup> and Regine von Klitzing<sup>\*a</sup>

Polyelectrolyte/surfactant mixtures of rigid monosulfonated poly(phenylene sulfone) (sPSO<sub>2</sub>-220) and tetradecyl trimethylammonium bromide (C<sub>14</sub>TAB) were investigated by surface tension, surface elasticity and foam film stability measurements. The results were compared to former measurements of polyelectrolyte/surfactant mixtures containing more flexible polyelectrolytes (PAMPS or PSS and C<sub>14</sub>TAB). For all polyelectrolyte/surfactant mixtures an increased surface adsorption in comparison to the pure surfactant was detected. Moreover, sPSO<sub>2</sub>-220/C<sub>14</sub>TAB mixtures showed a much higher surface activity and foam film stability than mixtures with more flexible polyelectrolytes. The results presented give insight into the surface adsorption and foam film formation of rigid polyelectrolyte/surfactant mixtures. Therefore, this study helps to understand the role of polyelectrolyte backbone rigidity in the formation and stabilization of foam films made from polyelectrolyte/surfactant mixtures.

Received 5th April 2016,  
Accepted 8th June 2016

DOI: 10.1039/c6cp02256a

www.rsc.org/pccp

### Introduction

Foam properties are of interest for many industrial applications such as enhanced oil recovery, fire fighting and advanced material synthesis and are thus the subject of many investigations.<sup>1–3</sup> In some processes like fire fighting a foam is desired, while in others (*e.g.* in washing machines) foaming should be avoided, which shows the high importance of foam stability control. In order to manipulate the properties of a foam, it is essential to understand the behavior of the single building blocks, so-called foam films. One way to produce stable foam films is to mix polyelectrolytes and surfactants. When mixing the two compounds, highly surface-active complexes can form due to electrostatic interactions.<sup>4,5</sup> Polyelectrolyte/surfactant mixtures play an important role in cleaning products and cosmetics.<sup>6,7</sup>

Depending on the charge combination of the used polyelectrolytes and surfactants, either a Common Black Film (CBF) with a thickness of 10–100 nm, or a Newton Black Film (NBF) with a thickness below 10 nm is formed as the final state before film rupture.<sup>5,8</sup> CBFs are electrostatically stabilized due to the presence of surface charges, while NBFs are stabilized by steric repulsions of the adsorbed complexes. CBFs contain two surface layers with differing amounts of water between them, while NBFs

consist of only two layers of adsorbed molecules and their respective hydration shells. The thickness of the latter is roughly twice the surfactant lengths, corresponding to 4–5 nm for low molecular weight surfactants. All other liquid is pressed out of the film. Another phenomena, which can occur for foam films formed by polyelectrolyte/surfactant mixtures, is stratification. In the case of stratification, the film drains stepwise due to an oscillation of the disjoining pressure.<sup>9–12</sup> This oscillation is induced by a transient network of the polyelectrolyte chains in the film core and/or by the layering of micelles, respectively.

For polyelectrolyte/surfactant mixtures the influence of different parameters such as polyelectrolyte/surfactant type,<sup>8</sup> polyelectrolyte/surfactant ratio,<sup>13</sup> polyelectrolyte/surfactant hydrophobicity,<sup>14</sup> pH and surfactant head group<sup>15</sup> and ion specific effects<sup>16</sup> on the air/water interface and foam film properties were extensively investigated. However, for most of the investigated polyelectrolyte/surfactant mixtures the polyelectrolyte backbones were quite flexible, *e.g.* poly(acrylamido methyl propanesulfonate) (PAMPS)<sup>13</sup> and poly(styrene sulfonate) (PSS).<sup>14</sup> Both have an intrinsic persistence length ( $l_p$ ) of 1 nm. The difference between the two is that PSS is more hydrophobic while PAMPS is more hydrophilic, which leads to significantly differing adsorption behavior of the resulting polyelectrolyte/surfactant complexes.<sup>13,14,17</sup>

Only very little work has been done to investigate the influence of a more rigid polyelectrolyte backbone on the surface adsorption and foam film properties of polyelectrolyte/surfactant mixtures.<sup>9,18,19</sup> In detail, the influence of the polyelectrolyte backbone rigidity on stratification behavior<sup>9,19</sup> was investigated. In ref. 9 the stratification behavior for mixtures of PSS ( $l_p = 1$  nm) and xanthan ( $l_p = 150$  nm)

<sup>a</sup> Stranski-Laboratorium, Department of Chemistry,  
Technische Universität Berlin, Strasse des 17. Juni 124, D-10623 Berlin,  
Germany. E-mail: klitzing@mailbox.tu-berlin.de

<sup>b</sup> Max Planck Institute of Colloids and Interfaces, Am Muehlenberg 1,  
14424 Potsdam, Germany

with dodecyltrimethylammonium bromide ( $C_{12}$ TAB) was investigated. Despite the strong difference in the polyelectrolyte backbone rigidity the stratification behavior was very similar.<sup>9</sup> In ref. 19 mixtures of PAMPS, carboxymethyl-chitin, DNA or xanthan (with  $l_p$  of 1 nm; 5 nm; 50 nm and 150 nm) with nonionic surfactants were investigated. Stratification was found for flexible polyelectrolytes, while for rigid polyelectrolytes stratification was dependent on the viscosity of the system.<sup>19</sup> Furthermore, the adsorption of mixtures containing PAMPS, PSS, DNA or xanthan (with  $l_p$  of 1 nm; 1 nm; 50 nm and 150 nm) with  $C_{12}$ TAB on the air/water interface was investigated.<sup>18</sup> Here, it was found that for more rigid polyelectrolytes denser films are formed at the air/water interface. To conclude, the first two studies concentrate on the stratification phenomena, while the third one only determines the adsorption at the air/water interface. Hence, to our knowledge no study investigated fundamentally the influence of polyelectrolyte backbone rigidity on both surface adsorption and foam film properties of polyelectrolyte/surfactant mixtures so far.

To overcome this shortcoming, here a monosulfonated poly(phenylene sulfone) (sPSO<sub>2</sub>-220) was chosen as polyelectrolyte and investigated thoroughly by means of surface tension and surface elasticity measurements and disjoining pressure isotherms. Sulfonated poly(phenylene sulfones) are a novel class of polyelectrolytes,<sup>20,21</sup> which are of interest due to their high proton conductivity and their high thermal, thermo-oxidative and hydrolytic stabilities.<sup>20,22</sup> These properties make sPSO<sub>2</sub>-220 a promising material *e.g.* for fuel cells.<sup>23</sup> Dissipative particle dynamics (DPD) simulations have shown that the sPSO<sub>2</sub>-220's polyelectrolyte backbone is significantly stiffer as for example the polyethylene backbones of PAMPS or PSS.<sup>24,25</sup> Furthermore, due to the electron withdrawing sulfonyl group ( $-SO_2-$ ) the sulfonate group is especially acidic for sPSO<sub>2</sub>-220, which leads to high dissociation degrees of 54–61%,<sup>26,27</sup> in comparison to a dissociation degree of 33–38% for PSS or PAMPS.<sup>28,29</sup>

$C_{14}$ TAB was chosen as surfactant, as it is the shortest surfactant in the  $C_n$ TAB series that forms stable films on its own.<sup>1</sup> This makes it possible to investigate the whole concentration regime from films of pure surfactant solutions, over those which contain little polyelectrolyte to films with a high polyelectrolyte concentration. The latter can already show stratification behavior. However, it is not the focus of this study to further investigate stratification for rigid polyelectrolyte/surfactant mixtures. Thus, in order to avoid stratification it is crucial to adjust the polyelectrolyte concentration below its critical overlap concentration ( $c^*$ ) and the surfactant concentration below its critical micelle concentration (cmc). Otherwise, the effects of surface charges would be superimposed by stratification of the film.

The aim of this work is to study the influence of the backbone rigidity of the polyelectrolyte in a polyelectrolyte/surfactant mixture on its surface adsorption and foam film properties. The system has been investigated by means of surface tension, surface elasticity and foam film stability measurements. The results are compared with former measurements of more flexible polyelectrolyte/surfactant mixtures (with PAMPS<sup>13</sup> and PSS,<sup>14</sup> respectively). The three polyelectrolytes sPSO<sub>2</sub>-220, PAMPS and PSS have the same charged group. The difference between the two

flexible polyelectrolytes, PAMPS and PSS, is that PAMPS is more hydrophilic, while PSS is more hydrophobic.<sup>14</sup> By the comparison of the chosen rigid and flexible polyelectrolytes it is possible to clarify the influence of the polyelectrolyte backbone rigidity.

## Experimental section

### Materials and sample preparation

The surfactant tetradecyl trimethylammonium bromide ( $C_{14}$ TAB) was purchased from Sigma-Aldrich (Steinheim, Germany) and recrystallized three times in acetone with traces of ethanol. The purity of the surfactant was verified by surface tension measurements. Monosulfonated poly(phenylene sulfone) (sPSO<sub>2</sub>-220) was synthesized according to the guidelines in the literature.<sup>21</sup> It had a molecular mass of 100 000 g mol<sup>-1</sup> with Li<sup>+</sup> as counterion. The flexible polyelectrolytes PAMPS and PSS, which were used for comparison, had a molecular mass of 100 000 g mol<sup>-1</sup> and 70 000 g mol<sup>-1</sup>, respectively. The molecular structure of the chemicals and polyelectrolytes used in this study is shown in Fig. 1.

sPSO<sub>2</sub>-220 was diluted, the resulting solution pressed through a syringe filter of 0.2 μm and then centrifuged at 4000 rpm for 60 min. The supernatant was collected and again centrifuged (with 7500 rpm, 3 runs for 15 min, between the runs the supernatant was diluted with deionized water) against centrifugal filters (Amicon Ultra 10 K, Merck Millipore, Germany) to remove small ion impurities from synthesis. The supernatant sPSO<sub>2</sub>-220 was then freeze dried and afterwards rediluted for experiments. All sample solutions were prepared with a fixed  $C_{14}$ TAB concentration (10<sup>-4</sup> M) and different sPSO<sub>2</sub>-220 concentrations in deionized water (Milli-Q; total organic content = 4 ppb; resistivity = 18 mΩ cm). The sample solutions were prepared by combining equal volumes of sPSO<sub>2</sub>-220/ $C_{14}$ TAB stock solutions with twice the desired concentration of the respective substance. All glassware (except the foam film holder) was cleaned with the basic detergent mixture Q9 (Ferah Berlin GmbH) and rinsed thoroughly with water before use. The porous glass disc was flushed with ethanol and water for several times. Prior to each measurement the foam film holder was boiled for 4 h in water.

Static light scattering (SLS) was used to extract the intrinsic persistence length of sPSO<sub>2</sub>-220. Samples with different sPSO<sub>2</sub>-220

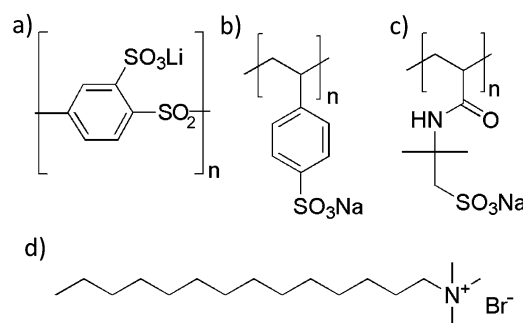


Fig. 1 Chemical structure of (a) sPSO<sub>2</sub>-220, (b) PAMPS, (c) PSS and (d)  $C_{14}$ TAB.

concentrations in water were analyzed as described earlier<sup>30</sup> and the molecular weight  $M_w$  and radius of gyration  $R_g$  were extracted. Data analysis was performed according to Gettinger *et al.*<sup>31</sup> The intrinsic persistence length can then be extracted.<sup>32</sup> The extracted intrinsic persistence length of sPSO<sub>2</sub>-220 is  $20 \pm 2$  nm, which is significantly higher than the persistence length of 1 nm for PAMPS and PSS.<sup>18</sup>

### Surface tension

The surface tension was measured with a K11 tensiometer (Krüss, Germany) using the du Noüy ring technique. Each sample solution was prepared 1 day beforehand. Prior to each measurement the sample solutions (with twice the desired concentrations) were mixed in a Teflon vessel (diameter 5 cm) and equilibrated for 2 h. The surface tension was measured at 25 °C until a constant value was recorded over more than 20 min.

### Surface elasticity

The surface elasticity of the sPSO<sub>2</sub>-220/C<sub>14</sub>TAB mixtures were measured at room temperature using a PAT1 (Sinterface Technologies, Berlin, Germany). The device created a pendant drop of the mixture at the tip of a capillary. This capillary was placed in a closed cuvette containing a small reservoir of sample solution to prevent evaporation. The drop was equilibrated for 2 h prior to each measurement. To determine the surface elasticity, harmonic oscillations of the drop surface were induced by a computer-controlled dosing system. Surface area  $A$  and surface tension  $\gamma$  were calculated as a function of time *via* drop shape analysis. The frequency of the drop oscillation was 0.1 Hz. The variation of surface area  $\delta A$  of the droplet causes a change of the surface concentration of the adsorbed surfactants. Surface expansion leads to a decrease in the surfactant surface concentration and thus to an increase in the surface tension  $\gamma$ . *Vice versa* the contraction of the surface results in a decrease of  $\gamma$ . At a given area variation the change in surface tension is a measure of the dilatational surface elasticity  $\varepsilon$ . The dilatational surface elasticity  $\varepsilon$  was calculated according to the following equation:

$$\varepsilon(\omega) = \varepsilon_r + i\varepsilon_i = \frac{\delta\gamma}{\delta \ln A} \quad (1)$$

The surface elasticity was calculated from the amplitude ratio of the oscillating surface tension and surface area, whereas the phase shift between the two determines the dilatational surface viscosity.<sup>33</sup>

### Thin film pressure balance

Disjoining pressure isotherms were measured with porous plates and the thin film pressure balance (TFPB) technique.<sup>34,35</sup> With this method free-standing horizontal liquid foam films can be investigated. Thus, information about interaction forces, thicknesses, drainage and stabilities of thin foam films are accessible. A full description of the setup can be found elsewhere.<sup>36</sup> In principle, the foam film is formed inside a hole of 1 mm in diameter, which is drilled into a porous glass disk. Before each measurement, the film holder was at least 2 h immersed in the sample solution for equilibration. Afterwards, it was pulled

out and left for surface equilibration for 2 h. All measurements were performed at 25 °C. The disjoining pressure isotherms were obtained by interferometrically measuring the foam film thickness  $h$ ,<sup>37</sup> while varying the pressure applied to the foam film. The equilibrium foam film thickness was measured after the intensity of the reflected light was constant for 20 min. All disjoining pressure isotherms shown within this study were averaged from at least three single measurements. Afterwards, the measured disjoining pressure isotherms were compared with model calculations according to the DLVO theory in order to determine the surface potential  $\Psi_0$ . The model calculations<sup>38,39</sup> were done by solving the non-linear Poisson–Boltzmann (PB) equation. Briefly, the ion profile between two planar surfaces is determined for 50 different distances in a regime between 0 and 100 nm. The planar surfaces have a surface potential  $\Psi_0$  and are separated by the distance  $D$ .

## Results

The focus of this study is to investigate the influence of the polyelectrolyte backbone rigidity on the adsorption behavior and foam film stability of oppositely charged polyelectrolyte/surfactant mixtures. Therefore, a mixture of the rigid polyelectrolyte sPSO<sub>2</sub>-220 and C<sub>14</sub>TAB was investigated with different techniques and the results were compared with former measurements using more flexible polyelectrolytes (PAMPS and PSS).<sup>13,14</sup> At first the results on the adsorption of sPSO<sub>2</sub>-220/C<sub>14</sub>TAB complexes at the air/water interface are presented. Secondly, the results on foam film stability are shown. In all experiments, the polyelectrolyte concentrations were varied between  $10^{-5}$  (mono)M and  $3 \times 10^{-3}$  (mono)M, whereas the C<sub>14</sub>TAB concentration was fixed at  $10^{-4}$  M. No turbidity and no precipitation of aggregates was detected, so homogeneous solutions are assumed for all mixtures. All experiments were performed after at least 2 h equilibration time. Longer equilibration time did not affect the adsorption or foam film properties. Therefore, it is assumed that the surface coverage is in equilibrium for all measurements.

### Characterization of the air/water interface

**Surface tension measurements.** Fig. 2 compares the surface tensions measured for mixtures of C<sub>14</sub>TAB (at a concentration of  $10^{-4}$  M) with different polyelectrolytes (sPSO<sub>2</sub>-220, PAMPS<sup>13</sup> and PSS,<sup>14</sup> respectively).

With increasing polyelectrolyte concentrations the surface tension isotherms can be divided into three distinctive regimes for all mixtures: polyelectrolyte concentrations below the bulk stoichiometric mixing point (BSMP), around the BSMP (at a polyelectrolyte concentration of  $10^{-4}$  (mono)M) and beyond the BSMP. The BSMP is the concentration at which, when assuming complete dissociation, the amount of positive charges from C<sub>14</sub>TAB and negative charges from sPSO<sub>2</sub>-220 is equal in bulk.

At lower polyelectrolyte concentrations, sPSO<sub>2</sub>-220/C<sub>14</sub>TAB mixtures already show a strong decrease in surface tension (around 39 mN m<sup>-1</sup>) in comparison to the pure surfactant (71 mN m<sup>-1</sup>). With increasing sPSO<sub>2</sub>-220 concentration the

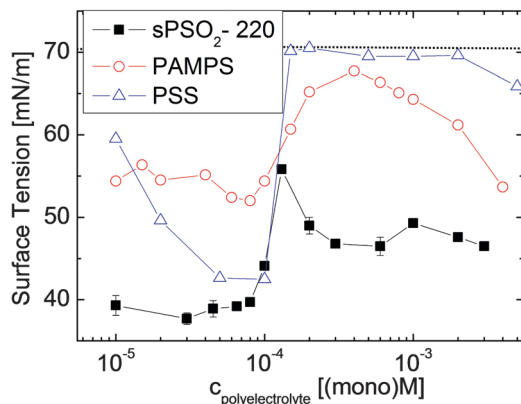


**Fig. 2** Surface tension of sPSO<sub>2</sub>-220/C<sub>14</sub>TAB solutions with fixed C<sub>14</sub>TAB concentration (10<sup>-4</sup> M) and variable sPSO<sub>2</sub>-220 concentration. For comparison the surface tension of the respective PAMPS/C<sub>14</sub>TAB (from ref. 13) and PSS/C<sub>14</sub>TAB (from ref. 14) mixtures is added. In this and the following figures the present measurements are plotted with closed symbols, while the former measurements are plotted with open symbols. The dotted line corresponds to the surface tension of pure C<sub>14</sub>TAB at 10<sup>-4</sup> M.

surface tension does not change significantly until the BSMP. In comparison, for PAMPS/C<sub>14</sub>TAB mixtures the surface tension is constant with increasing polyelectrolyte concentration, with surface tension values of around 55 mN m<sup>-1</sup>. For PSS/C<sub>14</sub>TAB mixtures the surface tension decreases to around 42.5 mN m<sup>-1</sup> with increasing polyelectrolyte concentration. At the BSMP and slightly beyond it the surface tension for sPSO<sub>2</sub>-220/C<sub>14</sub>TAB mixtures increases to slightly higher values (56 mN m<sup>-1</sup>). For PAMPS/C<sub>14</sub>TAB mixtures a strong increase to the value of pure surfactant was detected, while for PSS/C<sub>14</sub>TAB mixtures a very steep increase close to the pure surfactant value can be seen. At polyelectrolyte concentrations beyond the BSMP the surface tension of sPSO<sub>2</sub>-220/C<sub>14</sub>TAB mixtures stays constant around 47.5 mN m<sup>-1</sup>. For PAMPS/C<sub>14</sub>TAB mixtures the surface tension slightly decreases and for PSS/C<sub>14</sub>TAB mixtures it stays constant at values close to the pure surfactant value.

**Surface elasticity.** Investigations of the surface elasticity are useful for this research since they can be used to explain contradictions from surface tension and foam film stability results<sup>1,40</sup> as it is shown later. The surface elasticities of the three polyelectrolyte/surfactant mixtures are shown in Fig. 3.

The surface elasticity of pure C<sub>14</sub>TAB is 4 mN m<sup>-1</sup> at the concentration of 10<sup>-4</sup> M.<sup>13,41</sup> For sPSO<sub>2</sub>-220/C<sub>14</sub>TAB mixtures below the BSMP the surface elasticity rises slowly with increasing sPSO<sub>2</sub>-220 concentration. Close to the BSMP a plateau value at around 40 mN m<sup>-1</sup> is reached. At sPSO<sub>2</sub>-220 concentrations beyond the BSMP a strong increase in surface elasticity up to 115 mN m<sup>-1</sup> can be observed. At even higher concentrations the surface elasticity slightly drops and stays constant at 95 mN m<sup>-1</sup> with increasing concentration. For PAMPS/C<sub>14</sub>TAB mixtures the surface elasticity is roughly constant around 55 mN m<sup>-1</sup> at polyelectrolyte concentrations lower than the BSMP. Beyond the BSMP it drops to very low surface elasticity values around 5 mN m<sup>-1</sup>. Beyond a PAMPS concentration of 3 × 10<sup>-4</sup> (mono)M the surface elasticity linearly increases with increasing polyelectrolyte

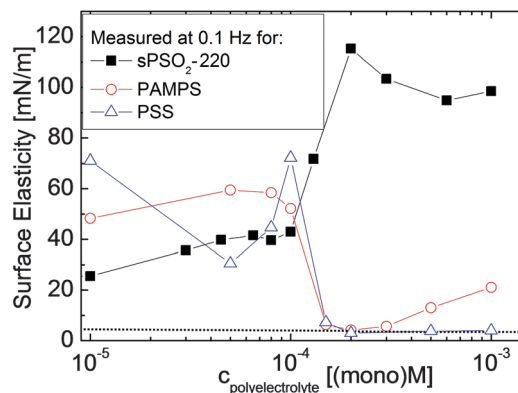


**Fig. 3** Surface elasticity of the sPSO<sub>2</sub>-220/C<sub>14</sub>TAB mixtures in comparison to PAMPS/C<sub>14</sub>TAB (taken from ref. 13) and PSS/C<sub>14</sub>TAB mixtures (taken from ref. 14). The colored lines are guidelines to the eyes only. The dotted line corresponds to the surface elasticity of pure C<sub>14</sub>TAB at 10<sup>-4</sup> M.<sup>13,41</sup> The error bars of the surface elasticity correspond to the size of the symbols.

concentration.<sup>13</sup> For PSS/C<sub>14</sub>TAB mixtures the surface elasticity is very discontinuous at polyelectrolyte concentrations below the BSMP. Even at a low polyelectrolyte concentration of 10<sup>-5</sup> (mono)M, the surface is very elastic (around 50 mN m<sup>-1</sup>). With increasing polyelectrolyte concentration the surface elasticity drops to 30 mN m<sup>-1</sup>. At 10<sup>-4</sup> (mono)M PSS, which corresponds to the BSMP, the surface elasticity is at its maximum of 72 mN m<sup>-1</sup>. With further increasing PSS concentrations the surface elasticity drops down to very low values of around 3 mN m<sup>-1</sup> and remains constant with increasing PSS concentration.<sup>14</sup>

At polyelectrolyte concentrations below the BSMP, sPSO<sub>2</sub>-220/C<sub>14</sub>TAB mixtures show a lower dilatational surface elasticity than the PAMPS/C<sub>14</sub>TAB and PSS/C<sub>14</sub>TAB mixtures. At polyelectrolyte concentrations slightly beyond the BSMP the dilatational surface elasticity of the mixtures varies strongly. While for sPSO<sub>2</sub>-220/C<sub>14</sub>TAB mixtures the dilatational surface elasticity increases at concentrations beyond the BSMP, for PAMPS/C<sub>14</sub>TAB and PSS/C<sub>14</sub>TAB mixtures it drops to the value of pure C<sub>14</sub>TAB.

### Properties of foam films – disjoining pressure isotherms

TFPB measurements give information about single foam film stabilities, being useful for understanding properties of macroscopic foams.

Fig. 4 shows disjoining pressure isotherms of sPSO<sub>2</sub>-220/C<sub>14</sub>TAB at different sPSO<sub>2</sub>-220 concentrations and fixed C<sub>14</sub>TAB concentrations (10<sup>-4</sup> M). Below the BSMP no stable films but only single values below 300 Pa of the disjoining pressures could be recorded for a certain concentration. With increasing sPSO<sub>2</sub>-220 concentration foam film stability decreases and at a concentration around 7 × 10<sup>-5</sup> (mono)M sPSO<sub>2</sub>-220 a point of destabilization is reached, where no stable foam film can be recorded at all. At the BSMP and beyond disjoining pressure isotherms could be measured. With increasing sPSO<sub>2</sub>-220 concentration both the foam film stability and the steepness of the slope of the disjoining pressure isotherms increases. The steeper slope with increasing sPSO<sub>2</sub>-220 concentration is in accordance with increasing ionic strength.

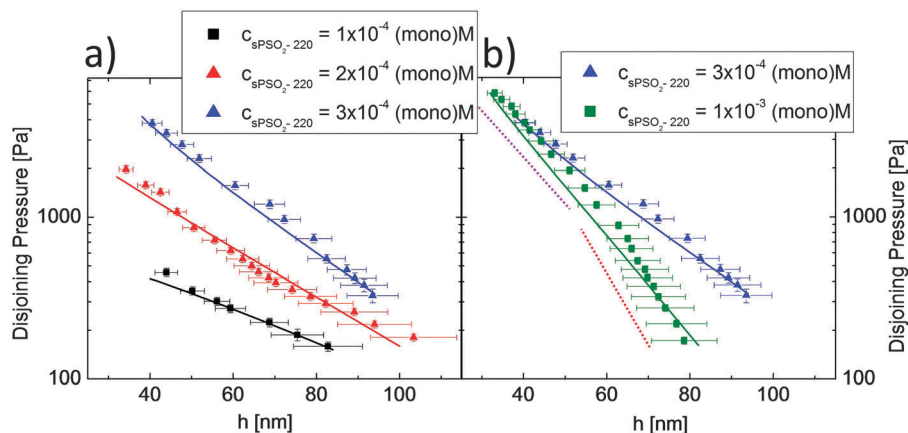


Fig. 4 Disjoining pressure isotherms of sPSO<sub>2</sub>-220/C<sub>14</sub>TAB solutions with fixed C<sub>14</sub>TAB concentration (10<sup>-4</sup> M) and variable sPSO<sub>2</sub>-220 concentration. The solid lines correspond to simulations at constant potential. In (a) three isotherms with lower sPSO<sub>2</sub>-220 concentrations and a continuous slope are shown. In (b) a kink can be seen in the second isotherm which has a sPSO<sub>2</sub>-220 concentration of 10<sup>-3</sup> (mono)M. Here the solid green line correspond to the simulations over the whole height range of the curve. The dotted lines correspond to the two different slopes of the curve and are shown offset from the data to enhance visibility. For comparison in (b) an isotherm from (a) is shown.

From the slope of the isotherms the Debye length  $\kappa_{\text{exp}}^{-1}$  and ionic strength  $I_{\text{exp}}$  were extracted (Table 1).<sup>36</sup> The experimentally determined ionic strength  $I_{\text{exp}}$  is compared in Table 1 to the maximum ionic strength  $I_{\text{max}}$  and the complex ionic strength  $I_{\text{complex}}$ .  $I_{\text{max}}$  is the ionic strength of the system when one assumes complete dissociation, while  $I_{\text{complex}}$  is the ionic strength of the system assuming complete dissociation and 1 : 1 binding between polyelectrolytes and surfactants. If the experimental ionic strength  $I_{\text{exp}}$  value is smaller than the complex ionic strength  $I_{\text{complex}}$  value dissociation is assumed to be incomplete.

**Table 1** Summary of the Poisson–Boltzmann simulations of the disjoining pressure isotherms of sPSO<sub>2</sub>-220/C<sub>14</sub>TAB films: surface potentials  $\Psi_0$ , the Debye length  $\kappa^{-1}$  and the ionic strength  $I_{\text{exp}}$  (extracted by an exponential fit to the data). For comparison the maximum ionic strength  $I_{\text{max}}$  (complete dissociation) and the complex ionic strength  $I_{\text{complex}}$  (complete dissociation and polyelectrolyte/surfactant complex formation in a 1 : 1 ratio) are shown. The former results for PAMPS/C<sub>14</sub>TAB and pure C<sub>14</sub>TAB are also added<sup>13</sup>

c sPSO <sub>2</sub> -220 [(mono)M]	$\Psi_0$ [mV]	$\kappa_{\text{exp}}^{-1}$ [nm]	$I_{\text{exp}}$ [M]	$I_{\text{max}}$ [M]	$I_{\text{complex}}$ [M]
1 × 10 <sup>-4</sup>	44	35.9	7.2 × 10 <sup>-5</sup>	2 × 10 <sup>-4</sup>	1 × 10 <sup>-4</sup>
2 × 10 <sup>-4</sup>	70	26.9	1.3 × 10 <sup>-4</sup>	3 × 10 <sup>-4</sup>	2 × 10 <sup>-4</sup>
3 × 10 <sup>-4</sup>	155	22.8	1.8 × 10 <sup>-4</sup>	4 × 10 <sup>-4</sup>	3 × 10 <sup>-4</sup>
1 × 10 <sup>-3</sup> (upper part)	168	15.8	4.1 × 10 <sup>-4</sup>	1.1 × 10 <sup>-3</sup>	1 × 10 <sup>-3</sup>
1 × 10 <sup>-3</sup> (whole isotherm)	182	13.6	5.0 × 10 <sup>-4</sup>	1.1 × 10 <sup>-3</sup>	1 × 10 <sup>-3</sup>
c PAMPS [(mono)M]	$\Psi_0$ [mV]	$\kappa^{-1}$ [nm]	$I_{\text{exp}}$ [M]	$I_{\text{max}}$ [M]	$I_{\text{complex}}$ [M]
1 × 10 <sup>-5</sup>	52	29	1.1 × 10 <sup>-4</sup>	1.1 × 10 <sup>-4</sup>	1 × 10 <sup>-4</sup>
5 × 10 <sup>-4</sup>	75	21.8	1.7 × 10 <sup>-4</sup>	6 × 10 <sup>-4</sup>	5 × 10 <sup>-4</sup>
1 × 10 <sup>-3</sup>	83	16	3.7 × 10 <sup>-4</sup>	1.1 × 10 <sup>-3</sup>	1 × 10 <sup>-3</sup>
Pure C <sub>14</sub> TAB [M]	$\Psi_0$ [mV]	$\kappa^{-1}$ [nm]	$I_{\text{exp}}$ [M]	$I_{\text{max}}$ [M]	$I_{\text{complex}}$ [M]
1 × 10 <sup>-4</sup>	70	29.3	1 × 10 <sup>-4</sup>	1 × 10 <sup>-4</sup>	1 × 10 <sup>-4</sup>

If the experimental ionic strength  $I_{\text{exp}}$  is higher than the complex ionic strength  $I_{\text{complex}}$  this indicates no 1 : 1 complexation.

To extract further information from the disjoining pressure isotherms they are simulated with the help of the nonlinear Poisson–Boltzmann equation at constant potential with the PB program version 2.2.1.<sup>38,39</sup> The results of this simulation and the comparison to former results from PAMPS/C<sub>14</sub>TAB mixtures<sup>13</sup> are listed in Table 1.

For all sPSO<sub>2</sub>-220/C<sub>14</sub>TAB mixtures  $I_{\text{exp}}$  is smaller than  $I_{\text{max}}$  and  $I_{\text{complex}}$ , which shows that the dissociation was not complete.  $I_{\text{exp}}$  values for sPSO<sub>2</sub>-220/C<sub>14</sub>TAB mixtures are higher than  $I_{\text{exp}}$  values for PAMPS/C<sub>14</sub>TAB mixtures, affirming the higher degree of dissociation of sPSO<sub>2</sub>-220 in comparison to PAMPS.<sup>27</sup>

In comparison to pure C<sub>14</sub>TAB, sPSO<sub>2</sub>-220/C<sub>14</sub>TAB mixture shows a reduced surface potential  $\Psi_0$  at polyelectrolyte concentration of 1 × 10<sup>-4</sup> (mono)M (44 vs. 70 mV). For higher sPSO<sub>2</sub>-220 concentrations the surface potentials of the sPSO<sub>2</sub>-220/C<sub>14</sub>TAB mixtures increase beyond the surface potential of pure C<sub>14</sub>TAB and reach values up to 180 mV. In comparison to PAMPS/C<sub>14</sub>TAB, sPSO<sub>2</sub>-220/C<sub>14</sub>TAB mixtures have a higher surface potential of roughly a factor of 2 at similar polyelectrolyte concentrations.

Interestingly, as shown in Fig. 4b, the disjoining pressure isotherm for a sPSO<sub>2</sub>-220 concentration of 1 × 10<sup>-3</sup> (mono)M shows a kink. To our knowledge such a kink in a disjoining pressure isotherm was only observed once before, for pure C<sub>14</sub>TAB close to the cmc.<sup>42</sup> For this isotherm with a sPSO<sub>2</sub>-220 concentration of 1 × 10<sup>-3</sup> (mono)M, both the whole isotherm and the upper part of the isotherm were simulated. The steeper lower part of the isotherm could not be simulated, since its slope was beyond the simulation range of the used software.

The disjoining pressure isotherms of PAMPS/C<sub>14</sub>TAB mixtures can be found in the literature.<sup>13</sup> Note that PSS/C<sub>14</sub>TAB mixtures did not show any stable foam films,<sup>14</sup> which can be contributed to a special destabilizing interaction of the aliphatic chain of longer trimethylammonium bromide surfactants and the benzene ring of PSS.<sup>17</sup> For the comparison of the absolute foam

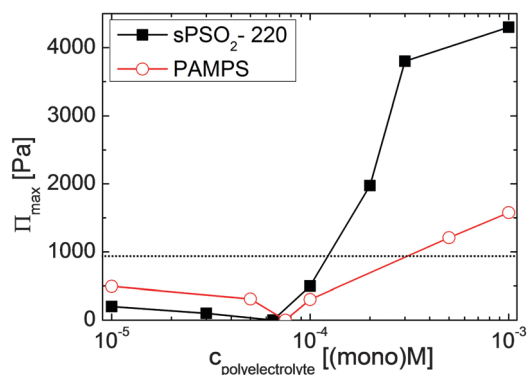


Fig. 5 The maximum disjoining pressure  $\Pi_{\max}$  before film rupture versus respective polyelectrolyte concentration for sPSO<sub>2</sub>-220/C<sub>14</sub>TAB films in comparison to PAMPS/C<sub>14</sub>TAB films (taken from ref. 13). The error bars correspond to the size of the symbols. The dashed line corresponds to the stability of a pure C<sub>14</sub>TAB film at 10<sup>-4</sup> M.

film stabilities of both mixtures, their maximum disjoining pressures  $\Pi_{\max}$  before foam film rupture are plotted in Fig. 5 against the concentration of sPSO<sub>2</sub>-220 and PAMPS,<sup>13</sup> respectively.

Qualitatively, both plots show a similar trend. Below the point of destabilization (slightly below the BSMP) the films are very unstable and show a decreasing stability with increasing polyelectrolyte concentration. However, for sPSO<sub>2</sub>-220/C<sub>14</sub>TAB mixtures it was only possible to measure stable disjoining pressure isotherms beyond a polyelectrolyte concentration of 10<sup>-4</sup> (mono)M, while PAMPS/C<sub>14</sub>TAB mixtures showed a stable foam film already at a polyelectrolyte concentration of 10<sup>-5</sup> (mono)M. At the point of destabilization (around  $8 \times 10^{-5}$  (mono)M for both sPSO<sub>2</sub>-220 and PAMPS) for both mixtures no stable foam film could be formed ( $\Pi_{\max} = 0$ ). At and beyond the BSMP stable films can be formed and the film stability increases with increasing polyelectrolyte concentration and rises beyond the stability of pure C<sub>14</sub>TAB films (around 900 Pa) at higher concentrations of both polyelectrolytes. The PAMPS/C<sub>14</sub>TAB films are slightly more stable below the point of destabilization, while beyond this point the sPSO<sub>2</sub>-220/C<sub>14</sub>TAB films are significantly more stable.

## Discussion

### Adsorption of sPSO<sub>2</sub>-220/C<sub>14</sub>TAB mixtures at the air–water interface

**Below the BSMP.** In the studied concentration regime the surface tension is already drastically reduced down to 39 mN m<sup>-1</sup>. With increasing sPSO<sub>2</sub>-220 concentration the surface tension stays constant up to the BSMP. In comparison to pure C<sub>14</sub>TAB (surface tension around 71 mN m<sup>-1</sup>) the sPSO<sub>2</sub>-220/C<sub>14</sub>TAB mixture shows a strongly reduced surface tension. This indicates that additional polyelectrolyte forms species in bulk or remains uncomplexed in the bulk phase. The synergistic lowering of the surface tension by sPSO<sub>2</sub>-220/C<sub>14</sub>TAB mixtures can be explained by the formation of surface active polyelectrolyte/surfactant complexes.<sup>5,13,14</sup> The formation of polyelectrolyte/surfactant complexes is energetically

favorable due to the decrease in electrostatic repulsion (between positively charged surfactant headgroups at the surface) and the increase in entropy due to the release of counterions.<sup>43,44</sup> Another explanation for the synergistic lowering of the surface tension would be a synergistic co-adsorption of polyelectrolyte and surfactant molecules.<sup>43</sup>

The surface tension of sPSO<sub>2</sub>-220/C<sub>14</sub>TAB mixtures at sPSO<sub>2</sub>-220 concentrations below the BSMP is significantly lower than for PAMPS/C<sub>14</sub>TAB (55 mN m<sup>-1</sup>) and PSS/C<sub>14</sub>TAB (60 mN m<sup>-1</sup>) mixtures with similar added amounts of the respective polyelectrolyte. Different reasons could be used to explain this differences in adsorption. The more flexible polyelectrolytes (PAMPS or PSS) might not reduce the surface tension as strongly, as they might coil and thus adsorb less on the surface, forming less dense films.<sup>13,14</sup> The formation of an especially dense film in case of a rigid polyelectrolyte was also observed in an earlier work.<sup>18</sup> Here, Stubenrauch *et al.* compared the surface tension and X-ray reflectivity of PAMPS/C<sub>12</sub>TAB and PSS/C<sub>12</sub>TAB mixtures to xanthan/C<sub>12</sub>TAB and DNA/C<sub>12</sub>TAB mixtures with a persistence length of 150 nm and 50 nm, respectively. The xanthan/C<sub>12</sub>TAB and DNA/C<sub>12</sub>TAB mixtures formed a very dense film (strong adsorption at the surface), while PAMPS/C<sub>12</sub>TAB and PSS/C<sub>12</sub>TAB mixtures formed a less dense film (weaker adsorption at the surface). Furthermore, earlier publications have shown that the degree of dissociation of sPSO<sub>2</sub>-220 is 54–61%<sup>27</sup> (depending on the measurement technique), which is higher than the degree of dissociation for flexible polyelectrolytes as PAMPS and PSS (around 33%).<sup>28,29</sup> Thus, there are more binding sites for C<sub>14</sub>TAB at sPSO<sub>2</sub>-220 than at PAMPS or at PSS. That leads to a stronger binding of C<sub>14</sub>TAB to sPSO<sub>2</sub>-220 and in turn to more surface active polyelectrolyte/surfactant complexes. Moreover, the charged groups in sPSO<sub>2</sub>-220 might be sterically easier accessible. For sPSO<sub>2</sub>-220 the charged group is in the polymer backbone, while for PAMPS and PSS it is in the polymer side chain. Due to their backbone flexibility PAMPS and PSS might coil, which would sterically block the charged group and hinder the binding of polyelectrolyte and surfactant. For sPSO<sub>2</sub>-220 the charged group is easily accessible due its position in the polyelectrolyte backbone and due to the backbone rigidity which hinders coiling. A schematic representation of the differences in adsorption of rigid/flexible polyelectrolytes with C<sub>14</sub>TAB independance of polyelectrolyte concentration is shown in Fig. 6.

In the polyelectrolyte concentration regime below the BSMP the surface elasticity of sPSO<sub>2</sub>-220/C<sub>14</sub>TAB mixtures increases from 20 mN m<sup>-1</sup> to 40 mN m<sup>-1</sup> with increasing sPSO<sub>2</sub>-220 concentration. Mixtures of PAMPS/C<sub>14</sub>TAB and PSS/C<sub>14</sub>TAB show a higher surface elasticity in this concentration regime (50–60 mN m<sup>-1</sup> and 30–70 mN m<sup>-1</sup>, respectively). As shown in the experimental part the surface elasticity describes how the surface tension reacts on the change of surface area. When surface active compounds move easily from the bulk phase to the surface this results in a low surface elasticity, which results in less stable foam films. When the exchange between the surface and the bulk phase is slow, this results in a high surface elasticity, which in turn results in higher foam stability.<sup>1,40</sup>

It is surprising that the surface elasticity for the sPSO<sub>2</sub>-220/C<sub>14</sub>TAB mixtures is lower than for PAMPS/C<sub>14</sub>TAB and PSS/C<sub>14</sub>TAB

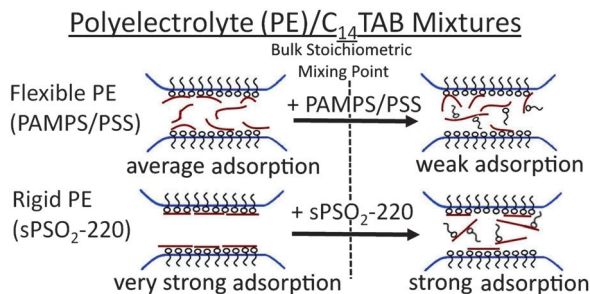


Fig. 6 Schematic representation of the differences in adsorption of rigid/flexible polyelectrolytes with C<sub>14</sub>TAB.

mixtures at low polyelectrolyte concentrations. This in opposition to the lower surface tension for sPSO<sub>2</sub>-220/C<sub>14</sub>TAB in comparison to PAMPS/C<sub>14</sub>TAB and PSS/C<sub>14</sub>TAB mixtures in this concentration regime and no simple explanation was found. On the one hand an explanation could be the difference in rotation time for the different polyelectrolytes. When the surface area is changed the polyelectrolytes need time to move and rotate accordingly. In ref. 19 it was shown that the rotation time of a polymer strongly depends on its persistence length. Hence, for flexible polyelectrolytes the system can react faster on the change in area, while for sPSO<sub>2</sub>-220 the slow rotation time might slow the reorientation and should thus increase surface elasticity. On the other hand sPSO<sub>2</sub>-220/C<sub>14</sub>TAB adsorbs stronger due to the stronger interaction as discussed earlier, the drag to the surface is stronger, hence resulting in faster exchange and lower surface elasticity values. As the surface elasticity for sPSO<sub>2</sub>-220/C<sub>14</sub>TAB mixtures is lower than for more flexible polyelectrolytes, the stronger interaction seems to be crucial.

**At the BSMP.** At and slightly beyond the BSMP sPSO<sub>2</sub>-220/C<sub>14</sub>TAB mixtures show an increase in surface tension. This increase is characteristic for polyelectrolyte/surfactant mixtures and its origin was discussed extensively elsewhere.<sup>5,45–47</sup> Different explanations can be found in literature explaining this phenomena: the complexes loss of surface activity at chemical equilibrium<sup>46,48</sup> and depletion of the surface due to precipitation of complexes in bulk.<sup>47,49</sup> As mentioned, no precipitation was observed here for sPSO<sub>2</sub>-220/C<sub>14</sub>TAB mixtures. Thus, the latter cause can be excluded.

An increase in surface tension was also observed for PAMPS/C<sub>14</sub>TAB and PSS/C<sub>14</sub>TAB mixtures at and slightly beyond the BSMP.<sup>13,14</sup> The increase in surface tension is the weakest for sPSO<sub>2</sub>-220/C<sub>14</sub>TAB mixtures, more pronounced for PAMPS/C<sub>14</sub>TAB mixtures and even stronger for PSS/C<sub>14</sub>TAB mixtures. The desorption of PSS/C<sub>14</sub>TAB complexes at PSS concentrations beyond the BSMP can be explained by an increasing hydrophilicity of the complex, since the aliphatic chain of C<sub>14</sub>TAB interacts with the benzene ring.<sup>17</sup> However, sPSO<sub>2</sub>-220 has a benzene ring as well and no surface depletion is observed. An explanation might be that due to the higher dissociation degree of sPSO<sub>2</sub>-220 more charged binding sites are available for C<sub>14</sub>TAB, which makes it more attractive for C<sub>14</sub>TAB to interact *via* the head group. Furthermore, for PSS the accessibility of the charge for C<sub>14</sub>TAB might be hindered as discussed earlier. This might lead to a preferred interaction with the benzene ring. The charge in

sPSO<sub>2</sub>-220 might be easier accessible for C<sub>14</sub>TAB due to its position in the backbone of the polyelectrolyte.

At the BSMP the surface elasticity of sPSO<sub>2</sub>-220/C<sub>14</sub>TAB mixtures strongly increases. This can be contributed to the fact that sPSO<sub>2</sub>-220 is now available in abundance in bulk, while less C<sub>14</sub>TAB is bound to each sPSO<sub>2</sub>-220 chain. That reduces sPSO<sub>2</sub>-220's drag to the surface. Thus, as more sPSO<sub>2</sub>-220 chains with less drag to the surface collect in bulk, the surface tension increases, while the replacement of chains on the surface is slowed down, leading to a higher surface elasticity. At the BSMP for PAMPS/C<sub>14</sub>TAB and PSS/C<sub>14</sub>TAB mixtures the surface elasticity strongly decreases, reaching the value of pure C<sub>14</sub>TAB. This is in accordance to surface tension measurements which show a strong increase in surface tension in this concentration regime.

**Beyond the BSMP.** Beyond the BSMP for sPSO<sub>2</sub>-220/C<sub>14</sub>TAB mixtures the surface tension remains constant at around 47.5 mN m<sup>-1</sup>. Additional sPSO<sub>2</sub>-220 does not further reduce the surface tension. This indicates that additional polyelectrolyte does not form surface active species. For PAMPS/C<sub>14</sub>TAB mixtures at first the surface tension increases with increasing polyelectrolyte concentration, then it decreases again. This is explained by the formation of PAMPS/C<sub>14</sub>TAB complexes in bulk up to a concentration of 5 × 10<sup>-4</sup> (mono)M PAMPS. Beyond this concentration the PAMPS adsorbs again at the surface.<sup>13</sup> For PSS/C<sub>14</sub>TAB mixtures the surface tension stays close to the water value with increasing PSS concentration, which is due to the formation of hydrophilic PSS/C<sub>14</sub>TAB complexes as mentioned earlier. All isotherms with polyelectrolyte concentrations above 10<sup>-3</sup> (mono)M show an already low or decreasing surface tension. This can be explained by the strong increase in ionic strength for such high polyelectrolyte concentrations. The high ionic strength leads to a screening of charges at the surface, which in turn leads to a stronger adsorption of both surfactant and polyelectrolyte.<sup>50</sup>

At sPSO<sub>2</sub>-220 concentrations beyond the BSMP the surface elasticity stays constant at high values with further increasing sPSO<sub>2</sub>-220 concentration. This is in accordance with constant surface tension values in this concentration regime. The high surface elasticity shows that in this concentration regime complexes are present both at the surface and in bulk. Beyond the BSMP PAMPS/C<sub>14</sub>TAB mixtures show a slight increase in surface elasticity which can be explained by the increased amount of adsorbed complexes. This is in accordance to a small decrease in surface tension in this concentration regime. PSS/C<sub>14</sub>TAB mixtures show a constant surface elasticity close to the value of pure C<sub>14</sub>TAB beyond the BSMP. This is in accordance to the surface tension measurements, which show little surface adsorption. Both high surface tension and low surface elasticity values can be explained by hydrophilic PSS/C<sub>14</sub>TAB complexes.

### Foam film properties of sPSO<sub>2</sub>-220/C<sub>14</sub>TAB mixtures

**Below the BSMP.** At polyelectrolyte concentrations below the BSMP the foam films of sPSO<sub>2</sub>-220/C<sub>14</sub>TAB mixtures are unstable. With increasing sPSO<sub>2</sub>-220 concentration foam film stability decreases further and at a concentration around 7 × 10<sup>-5</sup> (mono)M sPSO<sub>2</sub>-220 a point of destabilization is reached, where no stable foam film can be recorded at all. In contrast, for all PSS

concentrations no stable foam film can be recorded for PSS/ $C_{14}$ TAB mixtures.<sup>14</sup> The surface tension and surface elasticity values of PSS/ $C_{14}$ TAB mixtures beyond the BSMP indicates that there is almost no adsorption of PSS/ $C_{14}$ TAB complexes at the surface. Thus, in this section only results for sPSO<sub>2</sub>-220/ $C_{14}$ TAB and PAMPS/ $C_{14}$ TAB<sup>13</sup> mixtures are discussed. For PAMPS/ $C_{14}$ TAB mixtures foam films could be formed which showed a similar trend as sPSO<sub>2</sub>-220/ $C_{14}$ TAB films: unstable films at low polyelectrolyte concentrations and a point of destabilization slightly below the BSMP.

For low polyelectrolyte concentrations PAMPS/ $C_{14}$ TAB mixtures show more stable foam films than sPSO<sub>2</sub>-220/ $C_{14}$ TAB mixtures. This is counterintuitive to the results of surface tension measurements, which indicate that the adsorption at the air/water interface is stronger for sPSO<sub>2</sub>-220/ $C_{14}$ TAB than for PAMPS/ $C_{14}$ TAB mixtures. On the other hand the surface elasticity of sPSO<sub>2</sub>-220/ $C_{14}$ TAB is lower than the surface elasticity of PAMPS/ $C_{14}$ TAB mixtures. It is known for other systems that the foam film stability increases with increasing surface elasticity.<sup>1,40</sup>

It is counterintuitive that slightly below the BSMP no stable foam films can be formed for both mixtures, as in both cases surface tension and surface elasticity indicate a strong adsorption at the surface. This can be explained by the fact that for CBFs the film stabilization is not governed by the total adsorbed amount of polyelectrolyte/surfactant complexes, but by the net charge of the surface (as discussed extensively in earlier publications<sup>13,14,50</sup>). Thus, for a surface charge close to zero the foam film stability is the lowest. If one assumes that the foam film stability is governed by surface charge one would normally suppose that the point of destabilization is at the BSMP. Different reasons might lead to the shift of the point of destabilization from the BSMP to polyelectrolyte concentrations slightly lower than the BSMP. Firstly, the dissociation degree of  $C_{14}$ TAB might be below 100% in both mixtures, which would shift the BSMP to lower polyelectrolyte concentrations.<sup>5,13</sup> Secondly, the polyelectrolyte/surfactant mixing ratio at the surface might be different from that in the bulk, leading to a shift of the BSMP.<sup>5</sup> Thirdly, the pure air/water interface is slightly negatively charged.<sup>16</sup> Thus, a part of the positive charges of the surfactant is needed to compensate these charges. Hence, not all surfactant molecules are available to screen the charge of the polyelectrolyte molecules, which leads to shift of the point of destabilization to values slightly lower than the BSMP.

At the BSMP sPSO<sub>2</sub>-220/ $C_{14}$ TAB and PAMPS/ $C_{14}$ TAB mixtures form stable foam films.

**Beyond the BSMP.** Beyond the BSMP foam film stability of sPSO<sub>2</sub>-220/ $C_{14}$ TAB mixtures increases strongly with additional sPSO<sub>2</sub>-220. PAMPS/ $C_{14}$ TAB mixtures beyond the BSMP also show stable foam films. For polyelectrolyte concentrations beyond the BSMP surface tension measurements indicate that less complexes are at the surfaces for both mixtures, than for polyelectrolyte concentrations below the BSMP. This contradiction of increasing foam film stability and increasing surface tension can be contributed to the polyelectrolyte excess in bulk. Earlier publications have shown that not only the polyelectrolyte at the surface, but also that in the film bulk contribute to the

stabilization, by increasing the total net charge of the system.<sup>13,14,50</sup> Hence, increasing polyelectrolyte concentrations lead to increasing total net charge, which leads in turn to more stable foam films. The influence of the net charge of the system on the surface potential is also discussed later in this section.

While beyond the BSMP the foam film stability of both mixtures increases, foam films of sPSO<sub>2</sub>-220/ $C_{14}$ TAB mixtures are significantly more stable than their PAMPS/ $C_{14}$ TAB counterparts. This stronger increase in foam film stability is in accordance with surface tension measurements. Here, a stronger adsorption of sPSO<sub>2</sub>-220/ $C_{14}$ TAB than for PAMPS/ $C_{14}$ TAB mixtures is observed, which is contributed to the flat and effective adsorption at the air/water interface. Additionally, at concentrations beyond the BSMP, the higher surface elasticity of sPSO<sub>2</sub>-220/ $C_{14}$ TAB mixtures helps to explain the significantly higher foam film stability of sPSO<sub>2</sub>-220/ $C_{14}$ TAB in comparison to PAMPS/ $C_{14}$ TAB mixtures, since high surface elasticities are known to increase foam film stability.<sup>1,40</sup>

The Debye length  $\kappa^{-1}$  of sPSO<sub>2</sub>-220/ $C_{14}$ TAB mixtures was extracted. With increasing sPSO<sub>2</sub>-220 concentration the Debye length  $\kappa^{-1}$  decreases as the ionic strength increases. For sPSO<sub>2</sub>-220/ $C_{14}$ TAB the experimental ionic strength  $I_{\text{exp}}$  is below the complex ionic strength  $I_{\text{complex}}$ , which shows that the dissociation degree is not 100%. Former measurements on PAMPS/ $C_{14}$ TAB mixture also show a decrease of  $\kappa^{-1}$  with increasing polyelectrolyte concentration.<sup>13</sup> The decrease in Debye length  $\kappa^{-1}$  is stronger for sPSO<sub>2</sub>-220/ $C_{14}$ TAB than for PAMPS/ $C_{14}$ TAB mixtures, as the dissociation degree of sPSO<sub>2</sub>-220 is higher.

Furthermore, the isotherms were compared to Poisson-Boltzmann model calculations to extract the surface potential  $\Psi_0$ . In comparison to pure  $C_{14}$ TAB (at  $10^{-4}$  M) the sPSO<sub>2</sub>-220/ $C_{14}$ TAB mixture has a reduced surface potential at the BSMP (44 vs. 70 mV). The reason is the reduction of free charges due to binding of  $C_{14}$ TAB to sPSO<sub>2</sub>-220. However, the surface potential is only reduced by a factor of 1.6 for the sPSO<sub>2</sub>-220/ $C_{14}$ TAB mixture. That is in accordance with earlier assumptions that the surfactants degree of dissociation is not 100%, so that the lowest surface potential is reached at a polyelectrolyte concentration below  $10^{-4}$  (mono)M.<sup>13,14</sup> With increasing sPSO<sub>2</sub>-220 concentration the surface potential  $\Psi_0$  increases, as the ionic strength and polyelectrolyte surface adsorption increases as well. Former measurements also showed an increasing surface potential  $\Psi_0$  with increasing polyelectrolyte for PAMPS/ $C_{14}$ TAB mixtures.<sup>13</sup> However, the surface potentials  $\Psi_0$  are roughly a factor two higher for sPSO<sub>2</sub>-220/ $C_{14}$ TAB than for PAMPS/ $C_{14}$ TAB mixtures. This difference between sPSO<sub>2</sub>-220 and PAMPS might be due to two reasons: firstly, sPSO<sub>2</sub>-220 shows a stronger decrease in surface tension than PAMPS, hence either sPSO<sub>2</sub>-220 or  $C_{14}$ TAB adsorbs stronger at the air/water interface than for a PAMPS/ $C_{14}$ TAB mixture. Thus, for sPSO<sub>2</sub>-220/ $C_{14}$ TAB mixtures more polyelectrolyte and hence more charges might be adsorbed at the air/water interface as for PAMPS/ $C_{14}$ TAB mixtures. However, surface composition can not be investigated with the techniques used here. Therefore, the composition, the homogeneity and the structure of the film will be investigated in a further publication using neutron reflectometry (NR). Secondly, the higher dissociation degree



of sPSO<sub>2</sub>-220 as of PAMPS,<sup>27</sup> leads to higher ionic strength, which in turn leads to higher surface potentials. The difference in surface potential  $\Psi_0$  also helps to explain the higher foam film stability of sPSO<sub>2</sub>-220/C<sub>14</sub>TAB mixtures in comparison to PAMPS/C<sub>14</sub>TAB mixtures, as higher surface potential leads to more stable foam films.<sup>13,14,50</sup>

For a sPSO<sub>2</sub>-220 concentration of 10<sup>-3</sup> (mono)M a kink in the disjoining pressure isotherm was recorded. This is a rather unusual feature of a disjoining pressure isotherm. To our knowledge this was only observed in one other publication, where this phenomena was however not discussed.<sup>42</sup> Here, pure C<sub>14</sub>TAB was investigated at a concentration of 3.5 × 10<sup>-3</sup> M. Both our isotherm and the one from the literature share that the total ionic strength of the system is relatively large (concentrations beyond 10<sup>-3</sup> M) and that the kink in the isotherm is close to 1000 Pa. This kink could be a result of charge regulation. This phenomena describes the variation of the surface charge with the separation distance for overlapping double layers.<sup>51</sup> In our case the decrease of separation distance could lead to an expulsion of ions from the bulk phase to the film surface. This would result in a lower ionic strength and a longer Debye length  $\kappa^{-1}$  in bulk and a lower surface potential  $\Psi_0$  at the surface. For the evaluation of this isotherm with a kink both the complete isotherm and just the upper part of the isotherm was used. The difference in both results is rather small. The increase in Debye length  $\kappa^{-1}$  is indeed observed as the slope of the isotherm is less steep. Furthermore, the surface potential  $\Psi_0$  does also only marginally increase from a sPSO<sub>2</sub>-220 concentration of 3 × 10<sup>-4</sup> (mono)M to a concentration of 10<sup>-3</sup> (mono)M. Hence, the isotherms confirm that charge regulations play a major role in this system. For PAMPS/C<sub>14</sub>TAB mixtures at a polyelectrolyte concentration of 10<sup>-3</sup> (mono)M no kink was observed.<sup>13</sup> This can be explained by the higher ionic strength of sPSO<sub>2</sub>-220/C<sub>14</sub>TAB than of PAMPS/C<sub>14</sub>TAB mixtures, as a certain amount of charges are needed for the occurrence of the charge regulation phenomena. Charge regulation was extensively investigated with atomic force microscopy (AFM),<sup>51-53</sup> but to our knowledge not yet with TFPB. The kink in the disjoining pressure isotherm and the prerequisites for its appearance merits further investigations.

## Conclusion

This work shows that sPSO<sub>2</sub>-220/C<sub>14</sub>TAB mixtures adsorb stronger at the air–water interface than mixtures of more flexible polyelectrolytes (PAMPS or PSS with C<sub>14</sub>TAB). This is explained by the increase in polyelectrolyte backbone rigidity for sPSO<sub>2</sub>-220, which can lead to flat and effective adsorption at the surface. Furthermore, the higher dissociation degree of sPSO<sub>2</sub>-220 in comparison to PAMPS or PSS increases binding with the surfactant, and thus enhances surface adsorption. Hence, more complexes adsorb in a denser film at the surface in comparison to more flexible polyelectrolytes as PAMPS or PSS, which can form loops when adsorbing at the surface.

However, the stronger adsorption does not lead to more stable foam films below the BSMP. On the contrary, more stable foam

films are recorded for PAMPS/C<sub>14</sub>TAB than for sPSO<sub>2</sub>-220/C<sub>14</sub>TAB mixtures below the BSMP. This can be contributed to the comparatively low surface elasticity of sPSO<sub>2</sub>-220/C<sub>14</sub>TAB in comparison to PAMPS/C<sub>14</sub>TAB mixtures.

Beyond the BSMP, strong adsorption of sPSO<sub>2</sub>-220/C<sub>14</sub>TAB complexes lead to significantly more stable foam films than for PAMPS/C<sub>14</sub>TAB mixtures. This can be explained by the lower surface tension and the higher surface elasticity for sPSO<sub>2</sub>-220/C<sub>14</sub>TAB mixtures in comparison to PAMPS/C<sub>14</sub>TAB mixtures. Furthermore, surface potentials, which are decisive for stabilization of CBFs, are higher by a factor of 2 for sPSO<sub>2</sub>-220/C<sub>14</sub>TAB than for PAMPS/C<sub>14</sub>TAB mixtures. That confirms a high degree of dissociation for sPSO<sub>2</sub>-220 and leads to the high foam film stability and smaller Debye lengths of sPSO<sub>2</sub>-220/C<sub>14</sub>TAB mixtures.

The results found for the rigid sPSO<sub>2</sub>-220 might be generalized to other rigid polyelectrolytes, which are of importance in life science (e.g. DNA) or food technology (e.g. xanthan).

## Acknowledgements

The authors want to thank the group of Klaus-Dieter Kreuer (Max Planck Institute for Solid State Research, Stuttgart) for providing the sPSO<sub>2</sub>-220 sample. Furthermore, the authors thank Richard Campbell for helpful discussions. Martin Uhlig thanks Markus Witt and Anja Hörmann for help with the SLS measurements, Marieke Üzüüm for help with the manuscript and the DFG for financial support from SPP “Kolloid- und Verfahrenstechnik” 1273 Kl-1165/10.

## References

- 1 V. Bergeron, *Langmuir*, 1997, **7**, 3474–3482.
- 2 A. van der Net, A. Gryson, M. Ranft, F. Elias, C. Stubenrauch and W. Drenckhan, *Colloids Surf., A*, 2009, **346**, 5–10.
- 3 E. Rio, W. Drenckhan, A. Salonen and D. Langevin, *Adv. Colloid Interface Sci.*, 2014, **205**, 74–86.
- 4 D. Taylor, R. Thomas and J. Penfold, *Adv. Colloid Interface Sci.*, 2007, **132**, 69–110.
- 5 H. Fauser and R. von Klitzing, *Soft Matter*, 2014, **10**, 6903–6916.
- 6 J. M. Rodríguez Patino, C. Carrera Sánchez and M. R. Rodríguez Niño, *Adv. Colloid Interface Sci.*, 2008, **140**, 95–113.
- 7 J. F. Argillier, S. Zeilinger and P. Roche, *Oil Gas Sci. Technol.*, 2009, **64**, 597–605.
- 8 B. Kolarić, W. Jaeger, G. Hedicke and R. von Klitzing, *J. Phys. Chem. B*, 2003, **107**, 8152–8157.
- 9 R. v. Klitzing, A. Espert, A. Colin and D. Langevin, *Colloids Surf., A*, 2001, **176**, 109–116.
- 10 O. Theodoly, J. Tan, R. Ober, C. Williams and V. Bergeron, *Langmuir*, 2001, **17**, 4910–4918.
- 11 C. M. Beltrán and D. Langevin, *Phys. Rev. Lett.*, 2005, **94**, 1–4.
- 12 H. Fauser, M. Uhlig, R. Miller and R. von Klitzing, *J. Phys. Chem. B*, 2015, **119**, 12877–12886.
- 13 N. Kristen, V. Simulescu, A. Vüllings, A. Laschewsky, R. Miller and R. von Klitzing, *J. Phys. Chem. B*, 2009, **113**, 7986–7990.

- 14 N. Kristen, A. Vüllings, A. Laschewsky, R. Miller and R. von Klitzing, *Langmuir*, 2010, **26**, 9321–9327.
- 15 R. Petkova, S. Tcholakova and N. Denkov, *Colloids Surf., A*, 2013, **438**, 174–185.
- 16 N. Schelero and R. von Klitzing, *Curr. Opin. Colloid Interface Sci.*, 2015, **20**, 124–129.
- 17 C. Monteux, M. F. Llauro, D. Baigl, C. E. Williams, O. Anthony and V. Bergeron, *Langmuir*, 2004, **20**, 5367–5374.
- 18 C. Stubenrauch, P.-A. Albouy, R. v. Klitzing and D. Langevin, *Langmuir*, 2000, **16**, 3206–3213.
- 19 F. Kleinschmidt, C. Stubenrauch, J. Delacotte, R. von Klitzing and D. Langevin, *J. Phys. Chem. B*, 2009, **113**, 3972–3980.
- 20 M. Schuster, K.-D. Kreuer, H. T. Andersen and J. Maier, *Macromolecules*, 2007, **40**, 598–607.
- 21 M. Schuster, C. C. de Araujo, V. Atanasov, H. T. Andersen, K.-D. Kreuer and J. Maier, *Macromolecules*, 2009, **42**, 3129–3137.
- 22 C. C. de Araujo, K.-D. Kreuer, M. Schuster, G. Portale, H. Mendil-Jakani, G. Gebel and J. Maier, *Phys. Chem. Chem. Phys.*, 2009, **11**, 3305–3312.
- 23 K.-D. Kreuer and G. Portale, *Adv. Funct. Mater.*, 2013, **23**, 5390–5397.
- 24 C. Wang and S. J. Paddison, *J. Phys. Chem. A*, 2012, **117**, 650–660.
- 25 C. Wang and S. J. Paddison, *Soft Matter*, 2014, **10**, 819–830.
- 26 J. Smiatek, A. Wohlfarth and C. Holm, *New J. Phys.*, 2014, **16**, 025001.
- 27 A. Wohlfarth, J. Smiatek, K.-D. Kreuer, S. Takamuku, P. Jannasch and J. Maier, *Macromolecules*, 2015, **48**, 1134–1143.
- 28 G. S. Manning, *Annu. Rev. Phys. Chem.*, 1972, **23**, 117–140.
- 29 N. Gospodinova, E. Tomšík and O. Omelchenko, *Eur. Polym. J.*, 2016, **74**, 130–135.
- 30 L. Chiappisi, S. Prévost, I. Grillo and M. Gradzielski, *Langmuir*, 2014, **30**, 1778–1787.
- 31 C. L. Gettinger, A. J. Heeger, J. M. Drake and D. J. Pine, *J. Chem. Phys.*, 1994, **101**, 1673.
- 32 W. F. Reed, S. Ghosh, G. Medjahdi and J. Francois, *Macromolecules*, 1991, **24**, 6189–6198.
- 33 G. Loglio, P. Pandolfini, R. Miller, F. Ravera, M. Ferrari and L. Liggieri, *Novel Methods to Study Interfacial Layers*, Elsevier, Amsterdam, 2001.
- 34 D. Exerowa and M. Kruglyakov, *Foam and Foam Films—Theory, Experiment, Application*, Elsevier, Amsterdam, 1998.
- 35 K. J. Mysels and M. N. Jones, *Discuss. Faraday Soc.*, 1966, **42**, 42–50.
- 36 C. Stubenrauch and R. von Klitzing, *J. Phys.: Condens. Matter*, 2003, **1197**, R1197–R1232.
- 37 A. Sheludko, *Adv. Colloid Interface Sci.*, 1967, **1**, 391–464.
- 38 P. Linse, PB Version 2.2, 2009. See also [www.fkem1.lu.se/sm](http://www.fkem1.lu.se/sm).
- 39 C. Gutsche, U. Keyser, K. Kegler, F. Kremer and P. Linse, *Phys. Rev. E: Stat., Nonlinear, Soft Matter Phys.*, 2007, **76**, 1–7.
- 40 B. A. Noskov, *Curr. Opin. Colloid Interface Sci.*, 2010, **15**, 229–236.
- 41 C. Stubenrauch, V. B. Fainerman, E. V. Aksenenko and R. Miller, *J. Phys. Chem. B*, 2005, **109**, 1505–1509.
- 42 C. Stubenrauch, J. Schlarmann and R. Strey, *Phys. Chem. Chem. Phys.*, 2002, **4**, 4504–4513.
- 43 A. Asnacios, D. Langevin and J.-F. Argillier, *Macromolecules*, 1996, **29**, 7412–7417.
- 44 A. Asnacios, A. Espert, A. Colin and D. Langevin, *Phys. Rev. Lett.*, 1997, **78**, 4974–4977.
- 45 R. A. Campbell, A. Angus-Smyth, M. Yanez Arteta, K. Tonigold, T. Nylander and I. Varga, *J. Phys. Chem. Lett.*, 2010, **1**, 3021–3026.
- 46 A. Bahramian, R. K. Thomas and J. Penfold, *J. Phys. Chem. B*, 2014, **118**, 2769–2783.
- 47 Á. Ábrahám, A. Kardos, A. Mezei, R. A. Campbell and I. Varga, *Langmuir*, 2014, **30**, 4970–4979.
- 48 C. G. Bell, C. J. W. Breward, P. D. Howell, J. Penfold and R. K. Thomas, *Langmuir*, 2007, **23**, 6042–6052.
- 49 Á. Ábrahám, R. A. Campbell and I. Varga, *Langmuir*, 2013, **29**, 11554–11559.
- 50 H. Fauser, R. von Klitzing and R. A. Campbell, *J. Phys. Chem. B*, 2015, **119**, 348–358.
- 51 G. Trefalt, S. H. Behrens and M. Borkovec, *Langmuir*, 2016, **32**, 380–400.
- 52 I. Popa, P. Sinha, M. Finessi, P. Maroni, G. Papastavrou and M. Borkovec, *Phys. Rev. Lett.*, 2010, **104**, 228301.
- 53 I. Popa, G. Papastavrou and M. Borkovec, *Phys. Chem. Chem. Phys.*, 2010, **12**, 4863–4871.